Rotational and Translational Diffusion of Tobacco Mosaic Virus in Extended and Globular Polymer Solutions

Randy Cush, Derek Dorman, and Paul S. Russo*

Department of Chemistry and Macromolecular Studies Group, Louisiana State University, Baton Rouge, Louisiana 70803-1804

Received May 17, 2004; Revised Manuscript Received September 4, 2004

ABSTRACT: Depolarized dynamic light scattering is used to measure the translational and rotational diffusion of a rodlike probe, tobacco mosaic virus, in matrix solutions of dextran, an extended polymer with some branching, and globular Ficoll. Translation and rotation both decline almost exponentially as the concentration of either matrix rises. The ratio of rotational to translational diffusion is similar in dextran or Ficoll solutions and close to the values expected from continuum theories of the friction of rodlike particles. Reinforcing a continuum picture in which hydrodynamic effects surpass any due to topological constraints, the declines in rotational and translational motion are almost inversely proportional to the solution viscosity. Only modest and gradual deviations from Stokes−Einstein behavior are observed, even at high matrix concentrations. This stands in stark contrast to an earlier study by this group [*Macromolecules* **1997,** *30*, 4920−4926]. The difference may be traced to the subtle effects of optical rotation (dextran and Ficoll are chiral) on instrument alignment, coupled to the weak depolarization of the strongly scattering tobacco mosaic virus and the very slow rotations encountered at high matrix content. In optically inactive solutions, and even in optically active ones studied with the correct and tedious alignment, a particle the shape and size of tobacco mosaic virus can serve as an effective microrheological probe. Confirming this conclusion, the apparent microviscosity obtained by inverting rotational or translational diffusion coefficients reflected the molecular weight trend, at a particular concentration, of shear viscosity measured in a cone and plate device.

Introduction

Particle motion through complex fluids affects many commercial and natural processes, ranging from transport in living cells to the drying of paints and inks. The probe diffusion method targets such behavior at a fundamental level.[1−10] A particle (the probe) is followed as it moves through a suspension of other particles, a polymer solution, or a gel (the matrix). Many combinations of probe and matrix have been studied,[11−13] the most common probably being translational diffusion of spherical probes in solutions of random flight polymers. The results are sometimes evaluated according to the ability of the probes to behave as if they were in a continuum fluid. If diffusion decreases with concentration as fast as viscosity increases, the system is said to be under hydrodynamic control and exhibit Stokes−Einstein behavior. It was long ago envisioned[1,14] that probes much smaller than the "mesh" established by the constraining matrix may diffuse faster than expected. This could be taken as evidence for the importance of topological constraints, but their relative importance compared to hydrodynamic effects remains poorly understood in solutions.[15]

Little is known about rodlike probes in matrices composed of polymer chains[16−19] or spheres.[8] In the presence of strong topological constraints, the motion of an infinitely thin probe rod along its own axis might remain unhindered as polymer matrix is added, while end-over-end rotation is expected to slow dramatically.[20−22] Complete hydrodynamic control would suggest instead that translation and rotation decrease by about the same amount with addition of polymer matrix, reflecting viscosity increases. The testing of such a hypothesis poses difficult challenges, not the least of which is stability. Rods are poorly soluble. Although fears[23] that rods might aggregate even in demonstrably good solvents[24] probably reflect an incomplete understanding of the approach to the liquid crystalline phase,[25] the solubility of rods does indeed become more delicate when other macromolecules are added.[26] Nature provides several stable, electrically charged rods, but the aqueous environment complicates investigation by the popular and powerful dynamic light scattering method (DLS). This technique works best when the scattering of the matrix can be zeroed through refractive index matching with the solvent.[27−29] The refractive index of water is lower than that of any matrix polymer, so this is not possible for the important category of aqueous systems. (Low-refractive polymers and colloids can be closely matched in mixed aqueous solvents.[30−32])

Some years ago, this laboratory took advantage of the weak depolarized DLS signal of tobacco mosaic virus (TMV) to follow the apparent translation and rotation of that rodlike probe through solutions of the even more weakly depolarizing matrix polymer, dextran.[19] The polarizers effectively hid the matrix, providing an alternative to refractive index matching. The same strategy has been exploited by a few others using strongly depolarizing probes.[33−36] Only one molecular weight of dextran was studied. Throughout much of the concentration range, translation and rotation appeared to be under hydrodynamic control. Sudden transitions away from that behavior, in opposite directions for translation and rotation, almost coincided with large increases in viscosity at large concentrations. The transitions were interpreted as evidence for topological constraints, but it was concluded that the general utility of the depolarized DLS would require studies in additional systems. In this paper, additional molecular

* To whom correspondence should be addressed.

10.1021/ma0490294 CCC: $27.50
Published on Web 11/12/2004

weights of dextran are studied in addition to Ficoll, which is a globular polymer made by copolymerization of epichlorohydrin and sucrose. The sudden transitions observed earlier are subjected to much scrutiny on the basis of these results and subtle optical considerations.

Background

For depolarized measurements in Hv geometry (detector horizontal, incident light vertical) the homodyne intensity autocorrelation function is given by

$$g^{(2)}(t) = 1 + f\,|g^{(1)}(t)|^2 \tag{1}$$

in which f is an instrumental parameter, $0 < f < 1$, related to spatial coherence, detector dark count, and solvent scatter.[37] The electric field autocorrelation function, $g^{(1)}(t)$, is

$$g^{(1)}(t) = \exp(-\Gamma t) \tag{2}$$

where Γ is a decay rate. The decay rate for a cylindrically symmetrical, optically anisotropic, monodisperse, and inflexible scatterer is the sum of two terms:

$$\Gamma_{\mathrm{Hv}} = q^2 D_{\mathrm{T}} + 6D_{\mathrm{R}} \tag{3}$$

In this expression, D_{T} is the translational diffusion coefficient and q is the scattering vector magnitude ($q = 4\pi n \sin(\theta/2)/\lambda_0$, where n is the solution refractive index, θ is the scattering angle, and λ_0 is the incident light wavelength in vacuo). D_{R} is the end-over-end rotational diffusion coefficient. A series of measurements at different q yields both D_{T} and D_{R}. Equation 3 ignores coupling of translation and rotation.[38−41] The validity of this simple expression for TMV/dextran solutions was discussed previously[19] in terms of coupling constants between rotation and translational motion.[37,38,42] In principle, the DLS spectrum contains much other extractable information in interacting solutions[6,42] and also in dilute suspensions of very large rods at some scattering vectors.[40] The empirical result in this investigation is that eq 3 is obeyed by all solutions tested so far when the main depolarized DLS decay mode of dilute TMV dispersed in a nearly invisible matrix is isolated using Laplace inversion.[43,44] Both D_{T} and D_{R} are still regarded as *apparent* values approximating, at the low concentrations of the visible TMV probe particle, the translational self-diffusion and rotatory diffusion.

Materials and Methods

Young tobacco plants grown from seed (Ward Scientific or F. W. Richard Seed of Winchester, KY; the latter were Burley Tobacco Variety KY8959, Lot # 65-OTR8995A2IC-7, a strain that is highly susceptible to TMV). The best practice was to grow the plants in Jiffy Pellets (mostly peat moss). After transplanting to gallon-size containers, plants 6−10 in. high were infected by rubbing a dilute suspension of the U1 strain of TMV and a small amount of carborundum powder on their leaves. After several weeks, the leaves were harvested and frozen. The virus was purified by a method similar to that of Boedtker and Simmons;[45] details appear elsewhere.[18] Purified TMV solutions were stored at 4 °C at a concentration of about 30 mg/mL in a 0.01 M phosphate buffer, pH 7.5, containing 3 mM NaN_3 to prevent bacterial growth. TMV concentrations were determined using an absorbance of 3000 $cm^2\ g^{-1}$ at 260 nm.[45]

Polymer solutions were cleansed of particulates by diluting to about 3 wt % with dust-free water and filtering through a 0.1 μm Millipore Millex VV filter directly into dust-free DLS cells (13 mm test tubes with screw cap). The solutions were reconcentrated using a Savant Speedvac vacuum concentrator with a 0.2 μm Whatman filter fitted into the air inlet tube. Solutions were checked gravimetrically to ensure no polymer loss during the filtration step. This method consistently produced nearly dust-free concentrated polymer solutions without the usual difficulties of filtering highly viscous solutions. After addition of TMV stock, the solutions were mixed by slowly rotating samples at an angle using a homemade rotation device constructed from an ordinary hobby servo. All ternary solutions were held at 0.5 mg/mL TMV, using a TMV solution as the diluent to change polymer concentration.

The dynamic light scattering instrument was similar to one described previously.[46] A Coherent Innova 90 argon ion laser supplied about 200 mW at $\lambda_0 = 514.5$ nm. An ALV-5000 multibit correlator was used to obtain the correlation functions from measurements at 4 or 5 scattering angles ranging from 30° to 90°. Electronics consisted of a R928P Hamamatsu photomultiplier and a Pacific Precision model 126 pulse amplifier/discriminator. The sample holder temperature was controlled using a Lauda RM6 water bath to within ±0.1 °C.

Fluorescence photobleaching recovery (FPR) measurements of the optical tracer diffusion of dye-tagged TMV through dextran solutions followed procedures detailed elsewhere.[47]

The gel permeation chromatography/multiangle laser light scattering (GPC/MALLS) results for the dextrans appear in Table 1. The measured molecular weights and polydispersities often agreed with the vendor's advertised values. The higher molecular weight dextrans (>2 million advertised MW) were consistently found to have lower molecular weights than advertised. Data sheets accompanying these samples suggest that the advertised values were derived from measurements by conventional GPC (without light scattering detection) which is not an absolute method. Test runs of very sharp fractions of well-characterized pullulan standards consistently produced good agreement with vendor's data, so it is felt that the high-M dextrans may not be well characterized by the supplier. It is also possible that these largest dextrans experienced some shear degradation during GPC/MALLS, which may be consistent with the noticeably higher polydispersity values. As all runs were performed at the same flow rate, the dependence of measured values on flow rate was not determined. All subsequent data presented will be plotted using the values measured in this study, except in those cases where the molecular weight was too low to measure (the lowest four members in the PSS-dxtkit series). Even so, references to polymers will be by their advertised M's (e.g., 670K for dxt670K) in order to simplify comparison with other researchers using these same materials. The trend in tabulated radii of gyration, R_{g}, with molecular weight (not plotted) depends on the mass range and source of the dextrans. One does not generally observe the scaling relation $R_{\mathrm{g}} \sim M^{0.5-0.6}$ expected for random flight polymers, except over the narrow range ($143\,000 < M_{\mathrm{w}} < 389\,000$) for the three "PSS-dxtkit" samples that were large enough to permit reliable measurements of R_{g}. Dextran should generally be regarded as a lightly branched linear polymer.[48] Measurement of the globular Ficoll 400 (Pharmacia) yielded $M_{\mathrm{w}} = 428\,000 \pm 13\,000$ and a polydispersity $M_{\mathrm{w}}/M_{\mathrm{n}} = 4.3$. The root of the z-average of the squared radius of gyration was found to be 20 ± 3 nm.

Viscosities were measured in steady shear with a Brookfield LVTDCP cone and plate viscometer at the lowest reliable shear rates, ranging from 11.25 Hz for high concentrations to 450 Hz for low ones. Shear rate dependence was not observed. Oscillatory shear measurements on dextran samples of broader molecular weight distribution using a Rheometrics SR5000 at Tulane University also did not reveal significant dependence on oscillation frequency, even at the highest concentrations studied, up to 150 Hz. Further details of the rheology of dextran solutions are reported elsewhere.[48]

Results and Discussion

In agreement with the previous TMV/dextran study,[19] there was no sign of TMV aggregation in dextran or Ficoll solutions. Samples at any matrix concentration were stable over long periods. A typical plot of Γ vs q^2

Table 1. Weight-Average Molecular Weight, Polydispersity, and Root of the Weight Average and *z*-Average of the Squared Radius of Gyration of Dextrans by GPC/MALLS

advertised				measured			
catalog no.	lot no.	$M_w/10^3$	M_w/M_n	$M_w/10^3$	M_w/M_n	R_g (R_w)/nm	R_g (R_z)/nm
PSS-dxtkit[c]	Dxtp1	0.180	1.0	N/A			
PSS-dxtkit[c]	Dxtp2	0.342	1.0	N/A			
PSS-dxtkit[c]	Dxt1n1	1.2	1.18	N/A			
PSS-dxtkit[c]	Dxt5	5.2	1.6	N/A			
PSS-dxtkit[c]	Dxt12	12.0	1.56	12.0 ± 0.6	1.12		
PSS-dxtkit[c]	Dxt25	23.8	1.30	23.8 ± 0.3	1.05		
19412[a]	497100	40.0	1.5	41.6 ± 1.5	1.1		
PSS-dxtkit[c]	Dxt50	48.6	1.36	48.4 ± 2	1.07		
19413[a]	503606	75.0	1.5	77.0 ± 3.6	1.3		
PSS-dxtkit[c]	Dxt150	148	1.47	143 ± 6.8	1.22	10.3 ± 2	10.7 ± 1
19414[a]	410586	170	2.0	161 ± 6.4	1.7	17 ± 4	17 ± 3
PSS-dxtkit[c]	Dxt270	273	1.66	259 ± 7.4	1.16	14.2 ± 2	16 ± 2
PSS-dxtkit[c]	Dxt410	410	1.73	389 ± 24	1.28	18.2 ± 1	19.1 ± 1
D-1037[b]	90K-1897	413		370 ± 17	3.8	20 ± 3	21 ± 2
19415[a]	451049	600	1.7	536 ± 21	1.7	21 ± 2	24 ± 1
dxt670K[c]	*d*	676	1.94	647 ± 30	1.7	19 ± 4	22 ± 2
dxt2370K[c]	*d*	2370	1.61	1770 ± 34	1.3	24 ± 2	26 ± 2
dxt2750K[c]	*d*	2750	1.67	1550 ± 30	1.4	28 ± 2	30 ± 2

[a] Polysciences. [b] Sigma. [c] Polymer Standards Services. [d] Same as catalog no.

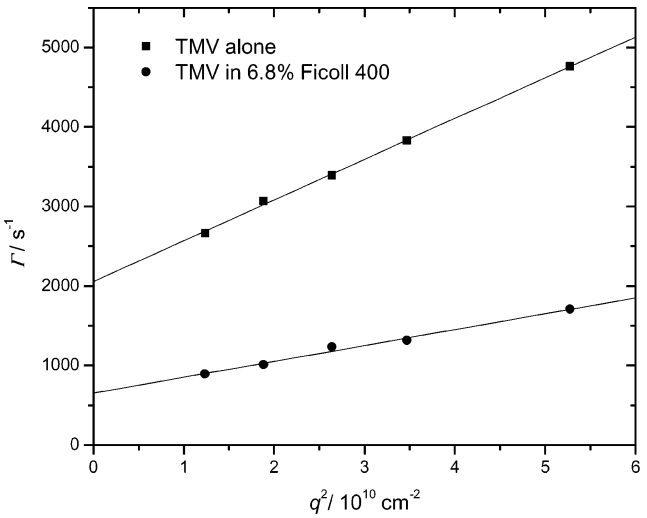

Figure 1. Decay rates from depolarized (Hv) DLS experiments. Upper points (■): dilute TMV; lower points (●): dilute TMV in 6.8% Ficoll 400.

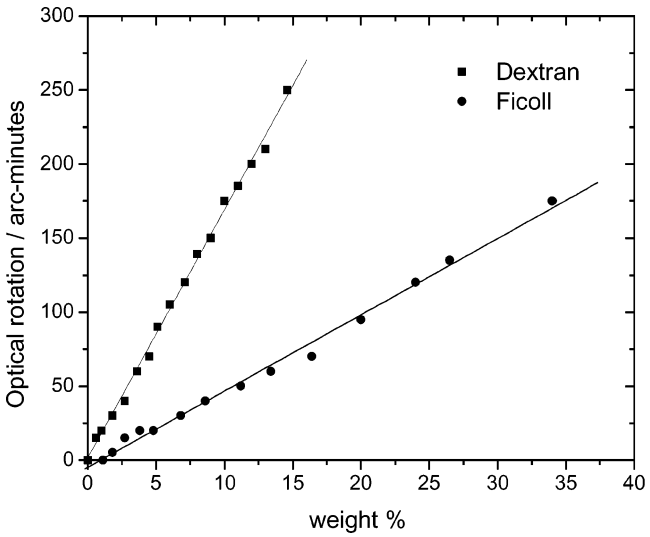

Figure 2. Optical rotation as a function of concentration for Dextran 670K (■) and Ficoll (●).

appears in Figure 1. As before, these plots were always linear, their intercepts yielding apparent rotational diffusion coefficients and their slopes apparent translational diffusion coefficients according to eq 3. As the matrix polymer (Ficoll in the case of Figure 1) increased, both transport coefficients were reduced. Experiments at high concentrations proved sensitive to details of the polarizer alignment, a fact not realized at the time of our previous study.[19] The problem was traced to the optical activity of the polymer matrix. An understanding of this effect, and how to compensate for it, is necessary in order to compare the present and previous results.

Figure 2 shows the optical rotation for dextran and Ficoll solutions as a function of concentration. To make these measurements, the input polarizer of the scattering instrument was set to vertical. To do this, the analyzer was rotated to horizontal by minimizing the scattering from a suspension of optically isotropic latex particles at 90° scattering angle. Then the input polarizer was added to the optical rail and rotated to vertical by minimizing the light transmitted through the still-horizontal detector at zero scattering angle. With the optically active sample inserted and the detector arm still set to zero scattering angle, the analyzer was rotated to extinguish (almost) the transmitted beam. The angular reading was compared to that required to extinguish an optically inactive sample (water). The rotation 2ϕ could be read to a precision of about 5 min, with an overall reproducibility of about half that. Proper vertical polarization of the incident beam at the center of the cylindrical cell is achieved when the input polarizer is cocked an angle $-\phi$. The desired horizontally depolarized scattered light rotates ϕ as it leaves the cell, so the analyzer is adjusted by ϕ to capture it. All measurements in this paper reflect the use of the proper alignment, except indicated data in Figure 3 where a comparison is drawn to the horizontal−vertical alignment used earlier.[19]

Failure to use the correct alignment causes significant errors for strongly scattering, but weakly depolarizing, particles that rotate slowly. This exactly describes TMV at high matrix concentrations, where the most interesting effects were observed in ref 19. Doty[49] measured the depolarization ratio (I_{Hv}/I_{Vv}) of TMV as only 0.0032, confirming the clever deductions of Lauffer[50] based on a study of streaming birefringence and visual observations of the scattering. Our own measurements suggest an even lower value. The weak depolarization of TMV, despite its axial ratio of about 17, reflects the absence of strong optical anisotropy in the protein and nucleic

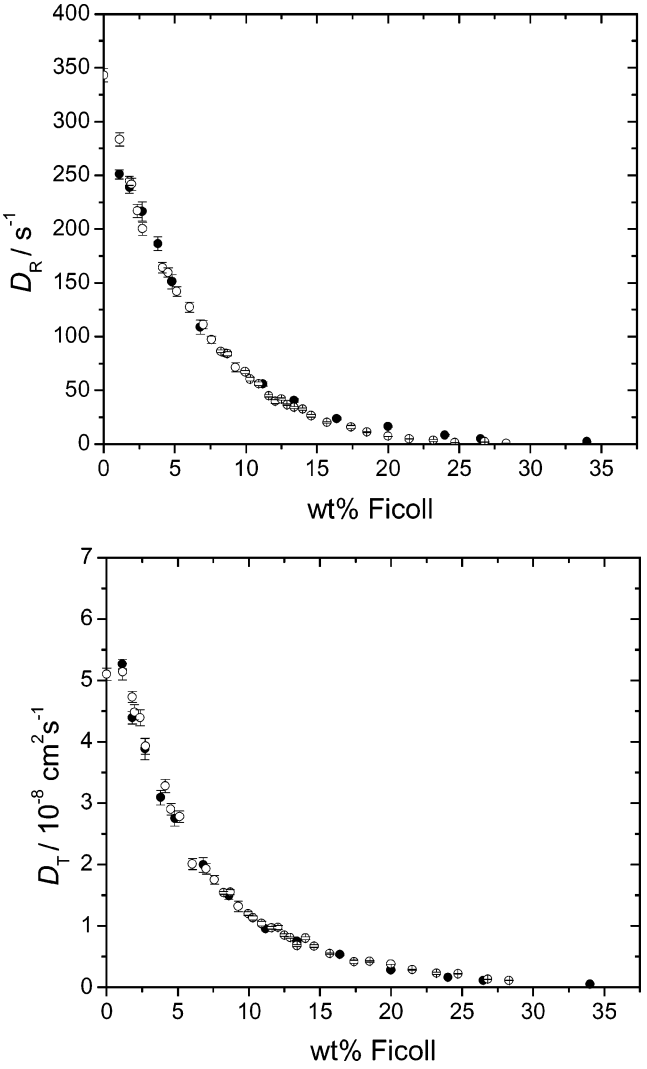

Figure 3. Apparent rotational (top) and translational (bottom) diffusion coefficient as a function of concentration with correct polarizer alignment (●) and incorrect alignment (○). Error bars are estimated from linear fits to the Γ vs q^2 plots.

acid building blocks. Geometric asymmetry does not confer optical anisotropy. If the polarizer−analyzer pair are in a standard vertical−horizontal alignment, as in the previous measurements,[19] some polarized scattered light can leak through and approach the level of the weakly depolarized light. The effect, which is analyzed in detail elsewhere,[18] is worst at $\theta = 0$ because the polarized scattered light continues the rotation suffered by the incident beam to exit the cell rotated by 2ϕ from the vertical, i.e., with a significant component in the horizontal direction of the analyzer. That component tends to produce a zero intercept in the Γ vs q^2 plots; the measured D_R is too small. The effect is nil at $\theta = 180°$ because the polarized scattered signal rotates by $-\phi$ on its way out of the cell and returns to the vertical. The wrong behavior at low angle, a contribution with zero intercept, and the right behavior at high angle result in a slope D_T that is too large. These effects, which become significant as D_R nears zero in systems characterized by depolarized scattering that is weak compared to the polarized, account for the sudden transitions observed previously.[19] The correct behavior will be revealed for the first time by the present measurements.

Figure 3 shows the decline of D_R and D_T with added Ficoll. The full points represent measurements with the correct alignment, while the more numerous open points

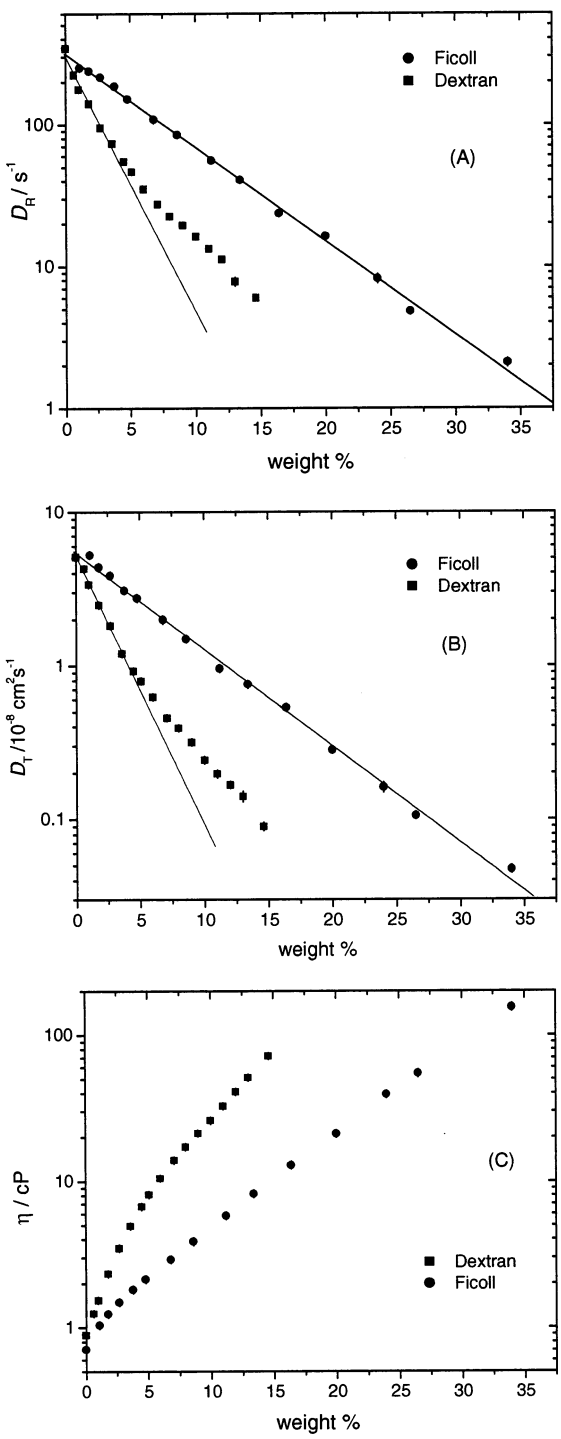

Figure 4. Apparent rotational (A) and translational (B) diffusion of TMV as a function of concentration of Ficoll (●) and Dextran 670K (■). Error bars are estimated from linear fits to the Γ vs q^2 plots. (C) Shear viscosities of Ficoll (●) and Dextran 670K (■). Errors estimated at 5%.

show results with the incorrect alignment. Although the difference is small, the incorrect alignment procedure consistently yields low values for D_R at high concentrations. Almost as consistently, it results in high values for D_T at elevated concentrations. Similar behavior was observed in dextran solutions (not shown).

Figure 4A,B and Table 2 display the results of correctly aligned experiments in dextran and Ficoll. With added Ficoll, TMV translation and rotation underwent simple exponential declines. Slightly more complex behavior was observed in dextran, but the

Table 2. Summary of Results for (a) TMV in Dextran 670000 (dxt670K) and (b) TMV in Ficoll 400

(a) TMV in Dextran 670000 (dxt670K)

dextran concn, %	D_T, 10^{-8} cm^2 s^{-1}	$\pm 10^{-8}$ cm^2 s^{-1}	D_R, s^{-1}	$\pm$ s^{-1}	η, cP	$\pm$ cP
0	5.10	0.10	343	6	0.890	0.045
0.63	4.29	0.19	224	10.1	1.25	0.06
1.0	3.39	0.16	176	8.6	1.54	0.08
1.8	2.49	0.04	141	2.2	2.33	0.12
2.7	1.82	0.07	94.9	3.7	3.49	0.17
3.6	1.20	0.04	73.2	2.1	4.95	0.25
4.5	0.92	0.01	54.8	0.7	6.74	0.34
5.1	0.79	0.03	46.4	1.8	8.12	0.41
6.0	0.62	0.02	34.9	1.0	10.5	0.53
7.1	0.46	0.02	27.4	1.2	13.9	0.70
8.9	0.39	0.01	22.6	0.71	17.2	0.86
9.9	0.32	0.01	19.5	0.65	21.3	1.1
10	0.24	0.01	16.2	0.74	26.0	1.3
11	0.20	0.01	13.4	0.62	32.5	1.6
12	0.17	0.01	11.2	0.42	40.8	2.0
13	0.14	0.01	7.81	0.58	51.1	2.6
14.6	0.09	0.01	6.00	0.29	71.8	3.6

(b) TMV in Ficoll 400

Ficoll concn, %	D_T, 10^{-8} cm^2 s^{-1}	$\pm 10^{-8}$ cm^2 s^{-1}	D_R, s^{-1}	$\pm$ s^{-1}	η, cP	$\pm$ cP
0	5.10	0.10	343	6	0.890	0.04
1.1	5.26	0.08	251	4	1.04	0.05
1.8	4.39	0.10	239	6	1.24	0.06
2.7	3.88	0.17	216	9	1.50	0.07
3.8	3.09	0.12	186	6	1.82	0.09
4.8	2.75	0.12	151	7	2.14	0.11
6.8	2.00	0.12	109	7	2.92	0.15
8.6	1.49	0.06	84.5	3.0	3.87	0.19
11.2	0.956	0.036	55.9	1.9	5.83	0.29
13.4	0.754	0.028	40.6	1.5	8.21	0.41
16.4	0.535	0.018	23.6	1.0	12.8	0.6
20.0	0.283	0.012	16.3	0.64	21.2	1.1
24.0	0.162	0.012	8.20	0.64	39.2	2.0
26.5	0.106	0.002	4.81	0.08	54.6	2.7
34	0.047	0.002	2.10	0.16	155	7.7

decrease of apparent rotational or translational diffusion always obeyed a stretched exponential form, $D \sim \exp(-\alpha c^{\nu})$ with modest stretching parameter, ν. The largest deviation of the stretching parameter from unity was $\nu \cong 0.7$ for D_R in dextran. Power law fits to concentration were unsuccessful for the TMV/dextran data in Table 2. Figure 4C displays the viscosity of dextran and Ficoll solutions; as expected, the lightly branched dextran produces a much higher viscosity at any given concentration than the globular Ficoll.

Few comparable experiments and relevant theoretical approaches have appeared. Building on the work of Tracy and Pecora,[51] Phalakornkul, Gast, and Pecora[8] measured the rotational diffusion of semiflexible poly(γ-benzyl-α-L-glutamate), PBLG, in colloidal spheres by transient electric birefringence (TEB). For sufficiently long PBLG molecules, they found strong and almost exponential decreases of D_R with concentration of the spheres. Unlike the present study, it was possible to test the dependence on rod length, which was found to be weaker than predicted by the theory of Pecora and Deutch.[52] Significant deviations from Stokes−Einstein behavior were found. Hill and Soane studied rotational diffusion of collagen in matrix solutions of very high molecular weight poly(ethylene oxide), a random flight polymer, also by TEB.[17,53] The primary theoretical contact was with an early paper by deGennes.[20] After extensions developed by the authors, results were in good agreement with expectations, showing very strong length and concentration dependences of power law

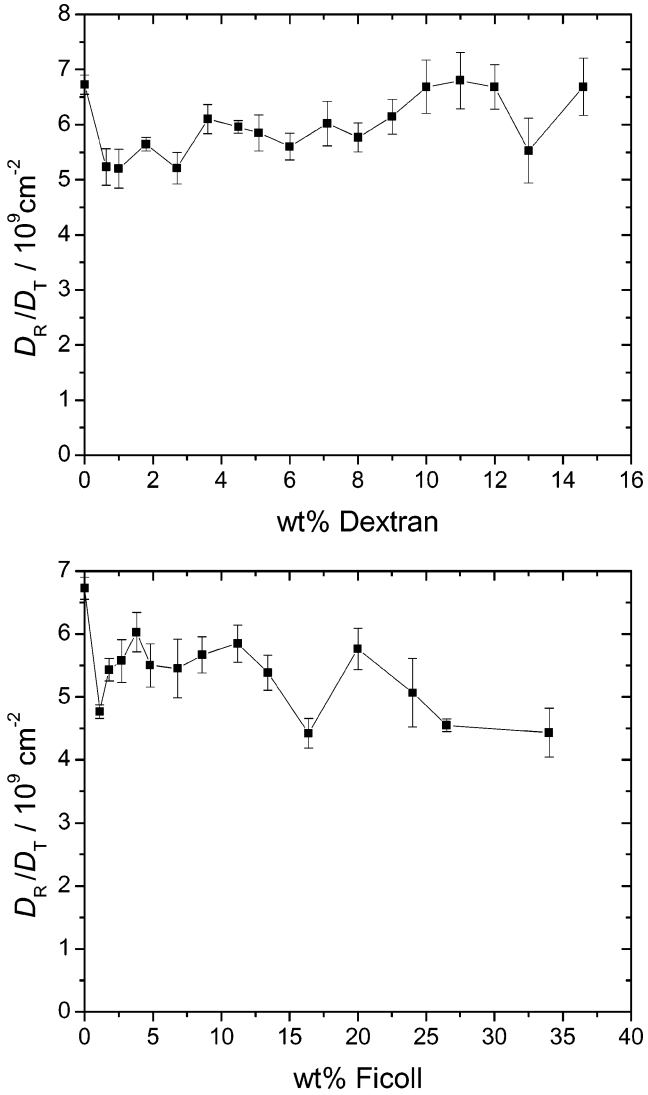

Figure 5. Ratio of apparent rotational and translational diffusion coefficients as a function of concentration of Dextran 670K (top) or Ficoll (bottom). Uncertainties are derived by propagating error estimates from the linear fits to the parent Γ vs q^2 data.

form. Rotational diffusion decreased according to $D_R \sim c_{matrix}^{-2}$ and did not follow the solution viscosity which, for the high molecular weight matrix used, approached $\eta \sim c_{matrix}^{5}$. Two collagen lengths were simultaneously present in the samples, and a very strong length dependence was found.

Good use can be made of the fact that two transport parameters, rotation and translation, are measured in the present study. Figure 5 shows the quotient of rotational and translational diffusion in dextran and Ficoll as a function of matrix concentration. In a simple fluid, such as a pure solvent, both D_R and D_T are inversely proportional to the viscosity. Detailed equations for D_R and D_T of cylindrical objects have been reviewed.[54,55] All of them will not be presented here, as some are rather detailed. The simplest Kirkwood−Riseman expressions[56] yield

$$\frac{D_R}{D_T} = \frac{\dfrac{3kT\ln(L/d)}{\pi\eta L^3}}{\dfrac{kT\ln(L/d)}{3\pi\eta L}} = \frac{9}{L^2} \approx 10^{10}\ \text{cm}^{-2} \qquad (4)$$

where k is Boltzmann's constant, T is the absolute temperature, and η is the viscosity. The value of 10^{10} cm^{-2} is obtained by using $L \approx 3000$ Å for TMV. If the more accurate expressions[54,55] of Broersma[57–59] or Tirado et al.[60] are substituted, using $d = 180$ Å, one obtains about 7.2×10^9 cm^{-2}. The measured quotient D_R/D_T is close to that expectation and remains almost constant over the entire range of concentrations in both the globular Ficoll matrix and the lightly branched dextran matrix. This suggests adherence to continuum hydrodynamics for TMV in these fluids, in agreement with lower concentrations of ref 19. The sudden transitions observed at elevated concentrations in ref 19 are absent in these improved measurements.

Our previous finding of sudden transitions in D_R/D_T, and their association with topological constraints, may have seemed reasonable because the transitions occurred just above the overlap concentration of the dextran matrix, where the ratio of TMV length to the measured transient network correlation length was large. It was thought that the anisotropic nature of the motion of a rod was revealing the existence of topological constraints in a way that spherical probes often do not. That behavior is entirely due to the misalignment caused by the optically active matrix, an effect that becomes very severe when D_R reaches low values in systems where the polarized scattering greatly exceeds the depolarized. When data gathered using the incorrect alignment procedure were used, sudden apparent transitions in D_R/D_T were again observed, even for globular Ficoll that cannot entangle in any traditional sense.

In conventional probe diffusion studies, where only the translational diffusion coefficient is measured, it is common to plot the product of ηD_T against c. Level behavior confirms adherence to the continuum Stokes–Einstein behavior. The Stokes–Einstein plots in Figure 6 confirm the impression from Figure 5 that deviations from continuum behavior are modest, at least compared to our previous study.

A concern with DLS is the relatively short distance scale over which it detects motions. The characteristic distance scale of DLS is $2\pi/q$ or about 0.2–0.8 μm for these measurements. These dimensions are similar to the length of the TMV particle itself, 0.3 μm. The distance scale, l, of the FPR measurements was 54–124 μm. Figure 7 demonstrates that D_T is almost the same on these disparate distance scales. The slightly larger values for FPR may reflect the self-assembled nature of TMV. If only a small percentage of the protein shell were to diffuse as detached unimers, the average diffusion would be raised. The similar values of D_T whether measured on short or long distance scales suggest that coupling between rotation and translation[37] does not severely corrupt the interpretation of the DLS results. As in the previous study, we still regard D_T and D_R as apparent values due to the coupling issue, but Figure 7 makes it likely that their physical meanings truly are translational and rotational diffusion.

Figure 8 demonstrates that D_T and D_R decrease with dextran molecular weight, at a constant concentration, according to power laws with similar exponents. In Figure 8C, the Broersma equations[57–59] for D_R and D_T have been solved for the apparent viscosity, or "microviscosity", η_μ, experienced by the TMV rods as they rotate and translate through dextran matrices all at 14.6 wt % but with different molar masses. Also shown are conventionally measured shear viscosities, but only for the PSS-dxtkit dextrans (supplies that would have enabled a direct comparison with DLS having been

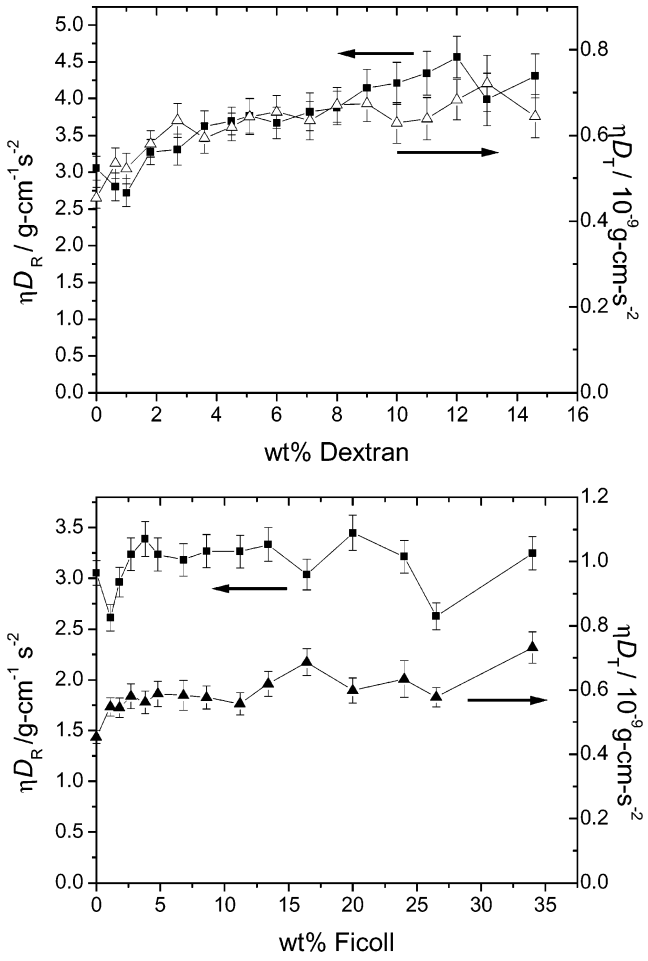

Figure 6. Stokes–Einstein plots for apparent TMV rotation (■) and translation (▲) in solutions Dextran 670K (top) or Ficoll (bottom). Uncertainties are derived by propagating estimated viscosity error and estimates from linear fits to the parent Γ vs q^2 data.

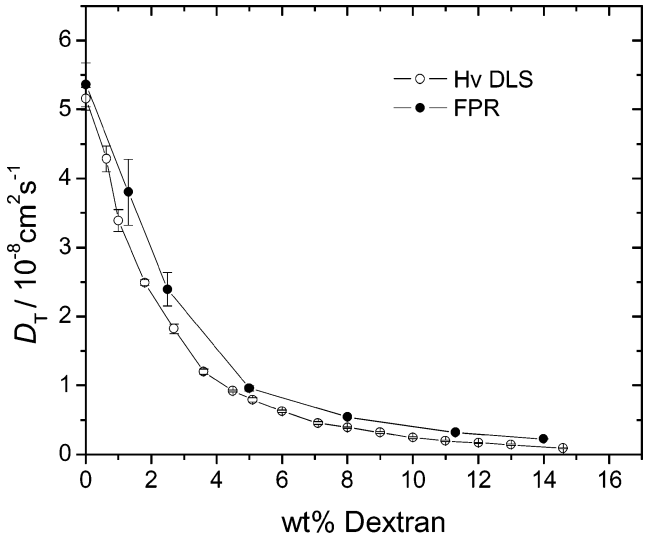

Figure 7. Comparison of TMV apparent translational diffusion coefficient from Hv DLS (○) and the L-TMV optical tracer self-translational diffusion coefficient from FPR (●) in solutions of Dextran 670K.

exhausted). The microviscosities are lower than the viscosities measured conventionally by almost a factor of 2 at high molecular weights. This implies slightly worse failures of the Stokes–Einstein relationship than seen in Figure 6 at high concentrations, but this may

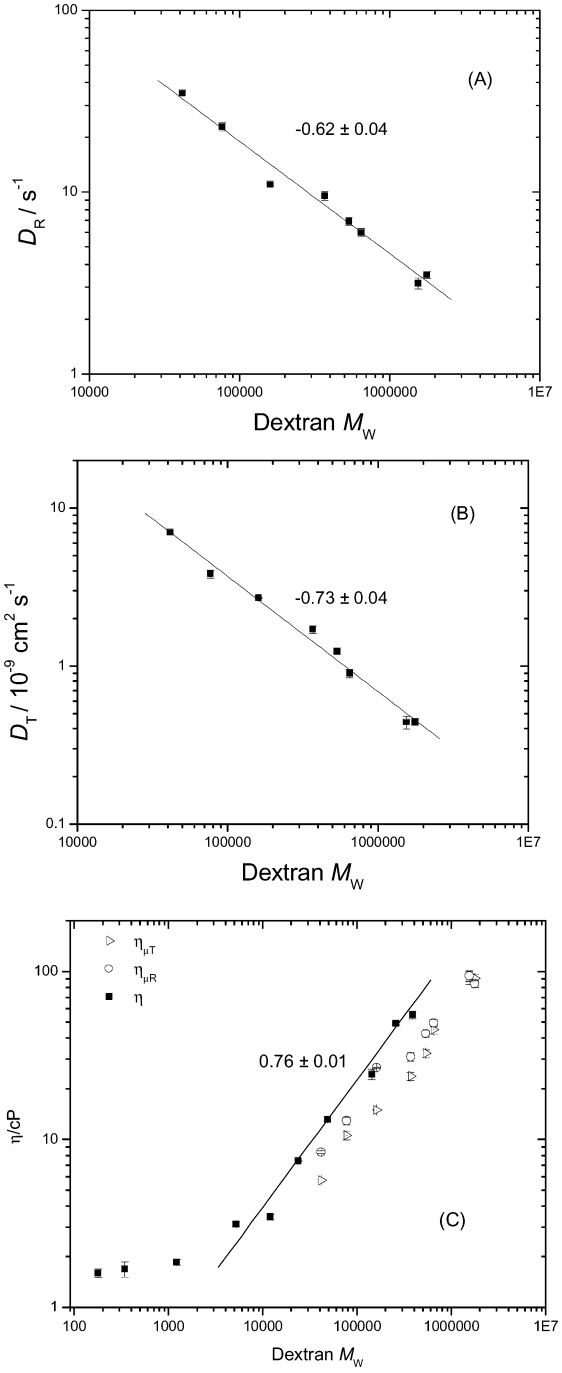

Figure 8. For dextran solutions at 14.6 wt %: dependence of apparent TMV rotational (A) and translational (B) diffusion from Hv DLS on dextran molecular weight and (C) macroscopic shear viscosity measured in a cone-and-plate viscometer for dextran solutions (■) together with apparent microviscosity determined using Broersma's equations from TMV rotational (—) and translational diffusion (χ) measurements by Hv DLS. Diffusion (microviscosity) uncertainties from (propagated from) linear fits to the Γ vs q^2 data. Uncertainties in macroscopic viscosity from experimentally observed range.

reflect the different dextran sources, especially the degree of branching, between the DLS and conventional viscosity experiments. The microviscosities do exhibit the same general behavior as the macroscopic viscosities, i.e., a power law with exponent similar in magnitude (opposite in sign) to those seen in Figure 8A,B. Figure 9 reveals that D_R/D_T values are not strongly sensitive to dextran molecular weight at the same fixed concentration, which is not surprising because that

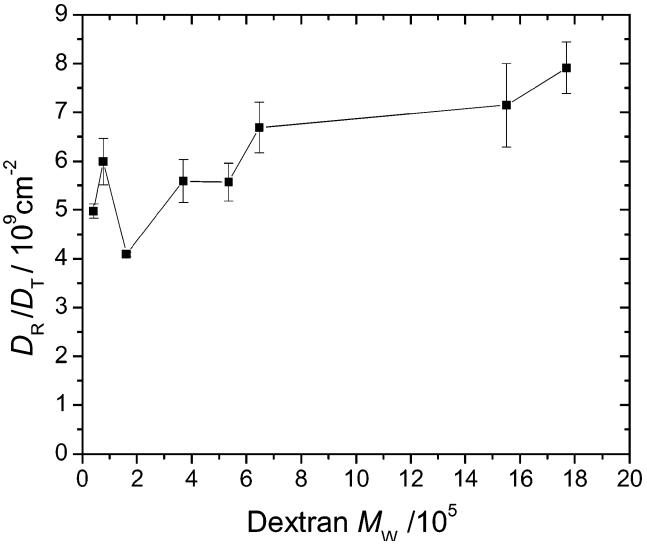

Figure 9. Ratio of apparent rotational and translational diffusion coefficients as a function of measured dextran molecular weight for solutions at 14.6 wt %. Uncertainties propagated from error estimates derived from linear fits to the Γ vs q^2 data.

quotient was little affected by changing the matrix architecture from globular to (lightly branched) chain, as shown in Figure 5.

Conclusion

This study features the very high stiffness of TMV as a probe, its good uniformity, and the ability of depolarized DLS to provide both translational and rotational diffusion simultaneously. Length variation is not included, and while our polymer matrices span an important range, they are less likely to entangle than those used by Hill and Soane.[17,53] Although the declines in both translational and rotational diffusion follow stretched exponential decay profiles, the stretching parameter was always modest. The declines are almost exponential. Power law behavior was not observed. Deviations from Stokes−Einstein behavior were modest, such that the diffusion of a rodlike particle the size of TMV may provide an effective means to measure or estimate the viscosity of fluids that are not readily measured by standard rheological instruments. Examples may include fluids in structured environments or polymeric solutions in supercritical solvents. No reader should be discouraged from such pursuits by the disagreements between this study and our previous attempt. The failings of the previous study required the convergence of high polarized scattering yet weak depolarized scattering by the probe rod, very slow rotational diffusion coefficients, and an optically active matrix polymer. In many cases, depolarized probe diffusion experiments are easy. A simultaneous, multiangle, multicorrelator scattering instrument could make them fast, too. Given the rapidly dropping price of correlator technology, this approach to microrheology may deserve additional development.

Acknowledgment. We thank Jonathan Strange for growing, infecting, and harvesting the tobacco plants. We thank Professor Daniel DeKee and members of his laboratory at Tulane University for confirming viscosity measurements by oscillatory shear over a wide range of shear rates. This work was supported by National

Science Foundation Award DMR-0075810 and a Louisiana Board of Regents Fellowship to R.C.C., who thanks Professor Nancy Thompson for her hospitality and the use of the Innova 90 laser source during an extended stay at the University of North Carolina—Chapel Hill. D.D. was supported as an NSF IGERT Fellow through Award DGE-9987603.

References and Notes

(1) Langevin, D.; Rondelez, F. *Polymer* **1978**, *19*, 875−882.
(2) Ogston, A. G. *Trans. Faraday Soc.* **1958**, *54*, 1754−1757.
(3) Onyenemezu, C. N.; Gold, D.; Roman, M.; Miller, W. G. *Macromolecules* **1993**, *26*, 3833−3837.
(4) Phillies, G. D. J. *Macromolecules* **1986**, *19*, 2367−2376.
(5) Turner, D. N.; Hallett, F. R. *Biochem. Biophys. Acta* **1976**, *451*, 305−312.
(6) Hanson, E. T.; Borsali, R.; Pecora, R. *Macromolecules* **2001**, *34*, 2208−2219.
(7) Lettinga, M. P.; van Kats, C. M.; Philipse, A. P. *Langmuir* **2000**, *16*, 6166−6172.
(8) Phalakornkul, J. K.; Gast, A. P.; Pecora, R. *J. Chem. Phys.* **2000**, *112*, 6487−6494.
(9) Kluijtmans, S. G. J. M.; Koenderink, G. H.; Philipse, A. P. *Phys. Rev. E* **2000**, *61*, 626−636.
(10) Koenderink, G. H.; Philipse, A. P.; Kluijtmans, S. G. J. M. *J. Phys.: Condens. Matter* **2000**, *12*, A339−A343.
(11) Phillies, G. D. J.; Streletzky, K. A. *Rec. Res. Dev. Phys. Chem.* **2001**, *5*, 269−285.
(12) MacKintosh, F. C.; Schmidt, C. F. *Curr. Opin. Colloid Interface Sci.* **1999**, *4*, 300−307.
(13) Gisler, T.; Weitz, D. A. *Curr. Opin. Colloid Interface Sci.* **1998**, *3*, 586−592.
(14) deGennes, P. G. *Scaling Concepts in Polymer Physics*; Cornell University Press: Ithaca, NY, 1979.
(15) Lodge, T. P.; Muthukumar, M. *J. Phys. Chem.* **1996**, *100*, 13275−13292.
(16) Clark, N. A.; Hurd, A. J.; Ackerson, B. J. *Nature (London)* **1979**, *281*, 57−60.
(17) Hill, D. A.; Soane, D. S. *J. Polym. Sci., Polym. Phys. Ed*. **1989**, *27*, 261−271.
(18) Cush, R. 2003. Ph.D. Thesis, Louisiana State University.
(19) Cush, R. C.; Russo, P. S.; Kucukyavuz, Z.; Bu, Z.; Neau, D.; Shih, D.; Kucukyavuz, S.; Ricks, H. *Macromolecules* **1997**, *30*, 4920−4926.
(20) deGennes, P. G. *J. Phys. (Paris)* **1981**, *42*, 473−477.
(21) Doi, M.; Edwards, S. F. *J. Chem. Soc., Faraday Trans. 2* **1978**, *74*, 560−570.
(22) Doi, M.; Edwards, S. F. *J. Chem. Soc., Faraday Trans. 2* **1978**, *74*, 918−932.
(23) Jinbo, Y.; Sato, T.; Teramoto, A. *Macromolcules* **1994**, *27*, 6080−6087.
(24) DeLong, L. M.; Russo, P. S. *Macromolecules* **1991**, *24*, 6139−6155.
(25) DuPre', D. B.; Samulski, E. T. Polypeptide Liquid Crystals. In *Liquid Crystals, the Fourth State of Matter*; Saeva, F. D., Ed.; Marcel Dekker: New York, 1979; pp 203−247.
(26) Flory, P. J. *Macromolecules* **1978**, *11*, 1138−1141.
(27) Lodge, T. P. *Macromolecules* **1983**, *16*, 1393−1395.
(28) Chu, B.; Wu, D.-Q. *Macromolecules* **1987**, *20*, 1606−1619.
(29) Martin, J. E. *Macromolecules* **1984**, *17*, 1279−1283.
(30) Koenderink, G. H. Rotational and Translational Diffusion in Colloidal Mixtures, Universiteit Utrecht, 2003.
(31) Hartl, W.; Beck, C.; Hempelmann, R. *J. Chem. Phys.* **1999**, *110*, 7070−7072.
(32) Pan, G. S.; Tse, A. S.; Kesavamoorthy, R.; Asher, S. A. *J. Am. Chem. Soc.* **1998**, *120*, 6518−6524.
(33) Piazza, R. *Phys. Scr.* **1993**, *T49A*, 94−98.
(34) Camins, B. C.; Russo, P. S. *Langmuir* **1994**, *10*, 4053−4059.
(35) Sohn, D.; Russo, P. S.; Davila, A.; Poche', D. S.; McLaughlin, M. L. *J. Colloid Interface Sci.* **1996**, *177*, 31−44.
(36) Koenderink, G. H.; Philipse, A. P. *Langmuir* **2000**, *16*, 5631−5638.
(37) Berne, B.; Pecora, R. *Dynamic Light Scattering*; Wiley: New York, 1976.
(38) Zero, K.; Pecora, R. *Macromolecules* **1982**, *15*, 87−93.
(39) Wilcoxon, J.; Schurr, J. M. *Biopolymers* **1983**, *22*, 849−867.
(40) Rallison, J. M.; Leal, L. G. *J. Chem. Phys.* **1981**, *74*, 4819−4826.
(41) Tracy, M. A.; Pecora, R. *Annu. Rev. Phys. Chem.* **1992**, *43*, 525−557.
(42) Phalakornkul, J. K.; Gast, A. P.; Pecora, R. *Macromolecules* **1999**, *32*, 3122−3135.
(43) Provencher, S. W. *Comput. Phys.* **1982**, *27*, 213−227.
(44) Provencher, S. W. *Comput. Phys.* **1982**, *27*, 229−242.
(45) Boedtker, H.; Simmons, N. S. *J. Am. Chem. Soc.* **1958**, *80*, 2550−2557.
(46) Russo, P. S.; Saunders, M. J.; DeLong, L. M.; Kuehl, S. K.; Langley, K. H.; Detenbeck, R. W. *Anal. Chim. Acta* **1986**, *189*, 69−87.
(47) Cush, R. C.; Russo, P. S. *Macromolecules* **2002**, *35*, 8659−8662.
(48) Doucet, G. Ph.D. Thesis, Louisiana State University, 2004.
(49) Doty, P.; Stein, S. J. *J. Polym. Sci.* **1948**, *3*, 763−771.
(50) Lauffer, M. A. *J. Phys. Chem.* **1938**, *42*, 935−944.
(51) Tracy, M.; Pecora, R. *Macromolecules* **1992**, *25*, 337−349.
(52) Pecora, R.; Deutch, J. M. *J. Chem. Phys.* **1985**, *83*, 4823−4824.
(53) Hill, D. A.; Soane, D. S. *J. Polym. Sci., Polym. Phys. Ed.* **1989**, *27*, 2295−2230.
(54) Zero, K.; Pecora, R. Dynamic Depolarized Light Scattering. In *Dynamic Light Scattering*; Pecora, R., Ed.; Plenum: New York, 1985.
(55) Russo, P. S. Dynamic Light Scattering from Rigid and Nearly Rigid Rods. In *Dynamic Light Scattering, the Method and Some Applications*; Brown, W., Ed.; Oxford: New York, 1993; pp 512−553.
(56) Riseman, J.; Kirkwood, J. G. *J. Chem. Phys.* **1950**, *18*, 512.
(57) Broersma, S. *J. Chem. Phys.* **1960**, *32*, 1626−1631.
(58) Broersma, S. *J. Chem. Phys.* **1960**, *32*, 1632−1635.
(59) Broersma, S. *J. Chem. Phys.* **1981**, *74*, 6989−6990.
(60) Tirado, M. M.; Martinez, C. L.; de la Torre, J. G. *J. Chem. Phys.* **1984**, *81*, 2047.

MA0490294